

# High-Performance Black Multicrystalline Silicon Solar Cells by a Highly Simplified Metal-Catalyzed Chemical Etching Method

Zhiqin Ying, Mingdun Liao, Xi Yang, Can Han, Jingqi Li, Junshuai Li, Yali Li, Pingqi Gao, and Jichun Ye

**Abstract**—A wet-chemical surface texturing technique, including a two-step metal-catalyzed chemical etching (MCCE) and an extra alkaline treatment, has been proven as an efficient way to fabricate high-efficiency black multicrystalline (mc) silicon solar cells, whereas it is limited by the production capacity and the cost cutting due to the complicated process. Here, we demonstrated that with careful control of the composition in etching solution, low-aspect-ratio bowl-like nanostructures with atomically smooth surfaces could be directly achieved by improved one-step MCCE and with no posttreatment, like alkali solution. The doublet surface texture of implementing this nanobowl structure upon the industrialized acidic-textured surface showed concurrent improvement in optical and electrical properties for realizing 18.23% efficiency mc-Si solar cells (156 mm  $\times$  156 mm), which is sufficiently higher than 17.7% of the solely acidic-textured cells in the same batch. The one-step MCCE method demonstrated in this study may provide a cost-effective way to manufacture high-performance mc-Si solar cells for the present photovoltaic industry.

**Index Terms**—Black silicon (b-Si), light trapping, metal-catalyzed chemical etching (MCCE), multicrystalline silicon (mc-Si), solar cell, surface texturing.

## I. INTRODUCTION

THE nanostructuring of silicon surfaces known as black silicon (b-Si) has attracted considerable attention for boosting the efficiency as well as reducing the manufacturing costs of solar cells via sufficient suppression of optical loss at front surface [1]–[7]. In particular, applying nanostructures at the mass production level has very important and practical significance

to multicrystalline silicon (mc-Si) solar cells, which constitute the largest part of the present photovoltaic, but an effective light-trapping technique is still lacking due to the random grain orientations. However, the conversion efficiencies of nanostructured b-Si solar cells are still far from satisfactory, especially for the conventional front-contacted solar cell structure with traditional antireflection coating (ARC) of silicon nitride ( $\text{SiN}_x$ ) [8]–[10]. To date, it is well acceptable that the surface recombination related to the larger surface area of the nanostructures and the Auger recombination at these highly doped nanostructures must be well controlled as low as possible, in order to achieve enhancement in efficiency [11]–[13].

In [9], the influence of the sheet resistance of nanostructures involving the emitter on carrier recombination have been deeply investigated, and the regimes of appreciated doping concentration for an emitter layer to mitigate the Auger recombination have been indicated. For the suppression of surface recombination, a straightforward choice is to design and fabricate novel silicon nanostructures with extremely low surface area but sufficient light harvesting. Our group reported a low-aspect-ratio honeycomb nanobowl structure, which is formed by first oxidizing silicon nanopores and then removing the oxide layer [12]. The enhancement in the surface area of the honeycomb nanobowl is only two times compared to the planar surface, but provides an overall reflection down to 2%, ranging from 400- to 900-nm wavelength. As an industry matching and cost-effective alternative, metal-catalyzed chemical etching (MCCE) was widely used to introduce secondary nanostructures upon the microsize bowl-like surface structures [2], [14]–[17], which were prefabricated by the standard acid texturing in conventional mc-Si solar cell industry. Ye *et al.* reported a novel nanoscale pseudopyramid structure formed by MCCE followed by NaOH modification and shown its effectiveness in improving efficiency [15]. Similar NaOH posttreatments have been utilized by other groups to lower the aspect ratio of the as-fabricated nanopores (caused by MCCE) well below 2 [14], [16], receiving improved blue spectral response and thus enhanced conversion efficiencies over 18% or even higher. Besides the standard acid texturing, the aforementioned b-Si needs several extra procedures: a two-step MCCE to fabricate nanopores, an immersion in dense  $\text{HNO}_3$  and buffered HF to dissolve the residual Ag and  $\text{SiO}_2$ , an NaOH treatment to lower the surface areas, and several times cleanings by deionized (DI) water to avoid cross contaminations. Obviously, it is a big challenge to successfully integrate so many batch processes into the well-established industrial streamline. Besides, the cost effectiveness and production consistency of

Manuscript received December 26, 2015; revised February 28, 2016; accepted April 12, 2016. Date of publication May 19, 2016; date of current version June 17, 2016. This work was supported by the Zhejiang Provincial Natural Science Foundation under Grant LY14F040005 and Grant LR16F040002; the National Natural Science Foundation of China under Grant 61404144, Grant 11304132, Grant 11304133, and Grant 61376068; the International S&T Cooperation Program of Ningbo under Grant 2015D10021; the “Thousand Young Talents Program” of China; and the One Hundred Person Project of the Chinese Academy of Sciences.

Z. Ying, M. Liao, X. Yang, C. Han, P. Gao, and J. Ye are with the Ningbo Institute of Material Technology and Engineering, Chinese Academy of Sciences, Ningbo 315201, China (e-mail: yingzhiqin@nimte.ac.cn; liaomd@nimte.ac.cn; yangx@nimte.ac.cn; hancan@nimte.ac.cn; gaopingqi@nimte.ac.cn; jichun.ye@nimte.ac.cn).

J. Li is with the Thin Film Laboratory, King Abdullah University of Science and Technology, Thuwal 23955-6900, Saudi Arabia (e-mail: Jingqi.li@kaust.edu.sa).

J. Li and Y. Li are with the Key Laboratory of Special Function Materials and Structure Design of the Ministry of Education and the School of Physical Science and Technology, Lanzhou University, Lanzhou 730000, China (e-mail: jshli@lzu.edu.cn; liyli@lzu.edu.cn).

Color versions of one or more of the figures in this paper are available online at <http://ieeexplore.ieee.org>.

Digital Object Identifier 10.1109/JPHOTOV.2016.2559779

the b-Si solar cells may also be affected when multiple chemical procedures were introduced. Therefore, although an average improvement of 0.3–0.5% absolute efficiency has been proven by this kind of wet-chemical b-Si technique, simplifying procedures to a large extent is of the most concern before it can be broadly accepted by photovoltaic industry.

In this paper, an improved technique with one-step MCCE processing and without alkaline posttreatment is demonstrated for fabricating the black mc-Si. The well-designed reaction solution contains an ultralow amount of  $\text{AgNO}_3$  (i.e., the one-tenth of the conventional MCCE), which can directly introduce uniform and shallow nanobowl-like structures upon the microbowl-like structures that were prefabricated via standard acid texturing on mc-Si surface. Our one-step MCCE process also has a polishing effect that offers atomically smooth surfaces to the nanobowl structures with potentially minimized defect density. In comparison with the standard acidic-textured case, the nanobowl/microbowl dual structures show not only improved light-trapping properties but enhanced minority carrier lifetime as well. As a result, the mc-Si solar cells ( $156 \text{ mm} \times 156 \text{ mm}$  in area) fabricated by our improved MCCE technique received an average conversion efficiency ( $\eta$ ) of 18.09% and short-circuit current ( $I_{\text{sc}}$ ) of 8.765 A, respectively, with 2.3% and 2.4% higher than that of reference cells.

## II. METHOD FOR EXPERIMENT

All experiments were performed on p-type mc-Si wafers with resistivity, thickness, and size of around  $2 \Omega\cdot\text{cm}$ ,  $180 \mu\text{m}$ , and  $156 \times 156 \text{ mm}^2$ , respectively. For fabricating the nanobowl/microbowl dual-structure textured solar cells, the wafers were first immersed into the standard acidic solution ( $\text{HNO}_3$ :  $\text{HF} = 2:1$ , at  $6^\circ\text{C}$ ) to form the microscale structures and were then dipped into  $\text{AgNO}_3/\text{HF}/\text{H}_2\text{O}_2$  mixed solution ( $\text{AgNO}_3$  below  $0.0001 \text{ mol}\cdot\text{L}^{-1}$ ,  $\text{HF}$  in  $0.05\text{--}5 \text{ mol}\cdot\text{L}^{-1}$ , and  $\text{H}_2\text{O}_2$  in  $1\text{--}10 \text{ mol}\cdot\text{L}^{-1}$ ) at room temperature for 1 min to create the nanoscale textures. It is worth noting that the consumption of  $\text{AgNO}_3$  here is only about one tenth over the previously reported two-step MCCE process. After that, the wafer was immersed into dense  $\text{HNO}_3$  solution for 3 min and then rinsed by DI water to remove the residual Ag nanoparticles. After the texturing process, phosphorous diffusion using  $\text{POCl}_3$  was performed at  $810^\circ\text{C}$  for 40 min to form the n-type emitters with a sheet resistance of around  $110 \Omega/\text{sq}$ . Standard rear-junction isolation and phosphorus silicon glass removal were subsequently performed in an industrial inline wet-chemical tool. With the aims of ARC and passivation, a stack of double-layer  $\text{SiN}_x$  film was deposited at  $477^\circ\text{C}$  using an inline direct plasma-enhanced chemical vapor deposition (PECVD) system, consisting of a 20-nm-thick bottom  $\text{SiN}_x$  layer with a refractive index of 2.25 and a 60-nm-thick top  $\text{SiN}_x$  layer with a refractive index of 1.95. Finally, the Ag front electrodes and Al back-surface contacts were formed by screen printing and cofiring in a lamp-heated belt furnace system. For comparison purpose, the solar cells based on the pure acidic texture and the acidic texture combined with previously reported nanopores structures by two-step MCCE [18]–[20] were also fabricated in the same batch.

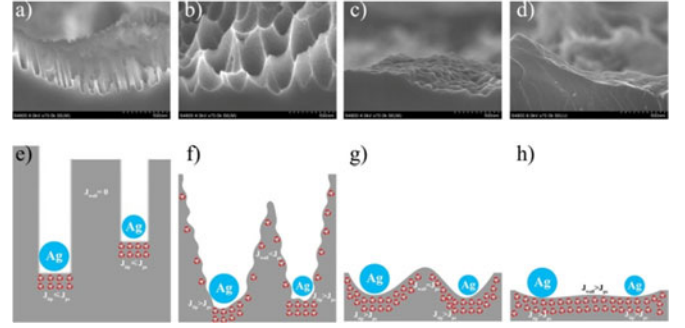


Fig. 1. (a)–(d) Cross-sectional SEM images and (e)–(h) schematics of the mechanism proposed for the formation of mc-Si samples after MCCE for  $\rho = 25, 20, 15$ , and  $7$ , respectively.

The textured structures of mc-Si wafers were analyzed by field emission scanning electron microscope (Hitachi S-4800). The crystal structures were determined by imaging with a high-resolution transmission electron microscope (HR-TEM, Tecnai F20). The surface reflections were examined by spectrophotometer (Helios LAB-rc) using an integrating sphere in the wavelength range of  $375\text{--}1075 \text{ nm}$ . The electrical characteristics of the mc-Si solar cells were investigated by photocurrent–voltage ( $I$ – $V$ ) measurement under the illumination of AM 1.5G using a solar-simulated light source. The external quantum efficiency (EQE) measurement in the wavelength of  $300\text{--}1075 \text{ nm}$  using a 300-W xenon lamp with a spot size of  $1 \times 3 \text{ mm}^2$  was calibrated with a silicon photodetector from Newport. The minority carrier lifetime was measured by microwave photoconductivity decay (WT-2000 PVN, Semilab).

## III. RESULTS AND DISCUSSION

In a typical one-step MCCE process, the deposition of metal catalysts and the dissolution of silicon are simultaneously happened in the mixed solution that contains  $\text{H}_2\text{O}_2$ ,  $\text{AgNO}_3$ , and  $\text{HF}$ . As shown in reaction (1), the introduction of  $\text{AgNO}_3$  gives rise to the generation of Ag on the silicon surface. The dense Ag nanoparticles (Ag NPs) could accelerate holes injection with the presence of oxidizing agent ( $\text{H}_2\text{O}_2$ ) and heavily shorten the diffusion distance of the injected holes in the vicinity of Ag NPs [1], [21], [22], as shown in reaction (2). Finally, the nanostructures are formed by the hole-induced silicon oxidation and the HF-driven dissolution of silicon oxides, referring to reaction (3). In brief, the final nanostructure configurations are mainly controlled by the density of the injected holes and their diffusion length, which are directly related to the ratios of the  $\text{H}_2\text{O}_2$  and  $\text{HF}$  once the amount of  $\text{AgNO}_3$  is fixed

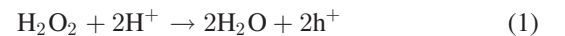


Fig. 1(a)–(d) showed the cross-sectional SEM images of the nanostructures formed on the acidic-textured Si surface by our one-step MCCE with different  $\rho$ , where  $\rho$  represented the molar ratio of  $[\text{HF}]/([\text{HF}] + [\text{H}_2\text{O}_2])$ . From Fig. 1(a)–(d), formation

of nanopores, enlarged craters, polished shallow nanobowls, and even flat surfaces are observed as  $\rho$  progressively decreases from 25%, 20%, and 15% to 7%. This phenomenon clearly showed that the decreasing proportion of HF induced both the enlargement of the pore diameter and the formation of nearly cone-shaped pores with Ag nanoparticles at the bottom, whereas the increasing in  $\text{H}_2\text{O}_2$  amount led to the rising of the opening angle of the craters [23]. The one-step MCCE process is actually known to be a mixed electroless and a chemical process. This electrochemical step implies that there are anode and cathode sites on the silicon surface with local cell currents that originate from holes injected in silicon by  $\text{H}_2\text{O}_2$ . In particular, the  $\text{H}_2\text{O}_2$  concentration can be considered as the equivalent of this current density in electrochemistry, while the HF concentration rules the surface chemistry and the dissolution of silicon oxides. For the convenience of discussion, the critical current density ( $J_{ps}$ ) was introduced, below or above which porous silicon formation or polishing occurs. The formation of structures for varying  $\rho$  can, thus, be schematically demonstrated in Fig. 1(e)–(h), respectively. For the case of  $\rho = 25\%$ , the current density was well below  $J_{ps}$  ( $J_{tip} < J_{ps}$ ), Ag nanoparticles dig pores into bulk Si, and the hole injection was localized at the Si/metal nanoparticle interface due to the catalytic properties of the metal. Thus, the Si was etched into porous Si, as shown in Fig. 1(a). With the decreasing of  $\rho$  ( $\rho = 20\%$ ), where the etching current was higher than critical current density ( $J_{tip} > J_{ps}$ ), an oxide layer was built at the Si/Ag interface due to the large  $\text{H}_2\text{O}_2$  concentrations. Then, the injected holes were diffusing from the pore tip to pore walls as a spread current, which is lower than  $J_{ps}$  ( $J_{walls} < J_{ps}$ ). Hence, the dissolution was isotropic and resulted in a polished surface at the pore tip and microporous Si formed on the pore walls, as shown in Fig. 1(b). While further decreasing  $\rho$  down to 15%, the etching current was still higher than the critical current density ( $J_{tip} > J_{ps}$ ), but the spread current may very close to  $J_{ps}$  ( $J_{walls} \approx J_{ps}$ ), in this case, a mixed regime of polishing and porous Si formation led to a polished surface not only at the pore tip but on the pore walls as well. For this reason, the etching surface was becoming much smoother [see Fig. 1(c)], causing a surface texture quite similar to the alkali treatment. Finally, when both the etching current and the spread current were sufficiently higher than the critical current density ( $J_{tip} > J_{ps}$ ,  $J_{wall} > J_{ps}$ , for  $\rho = 7\%$ ), where the oxidized layer thickened and covered the entire surface. Thus, the dissolution was isotropic, independent of metal nanoparticles location and resulted in a polished surface, as shown in Fig. 1(d).

In order to evaluate the light-harvesting characteristics of the aforementioned four structures, the reflectance in the wavelength range of 375–1075 nm was measured, as shown in Fig. 2(a). In contrast with the pure acidic textures, the as-fabricated hierarchical structures effectively reduced the reflectance over the entire band regions and exhibited the reduced average reflectance from 31.93%, 16.80%, 10.37%, and 4.85%, for the structures of  $\rho = 7\%$ , 15%, 20%, and 25%, respectively. The superior light-harvesting property of the hierarchical structures that fabricate under  $\rho = 7\%$ , 15%, 20%, and 25% could be attributed to two effects: the scattering effect of the microbowl-like structures (acidic texture) with a feature size of 2–6  $\mu\text{m}$

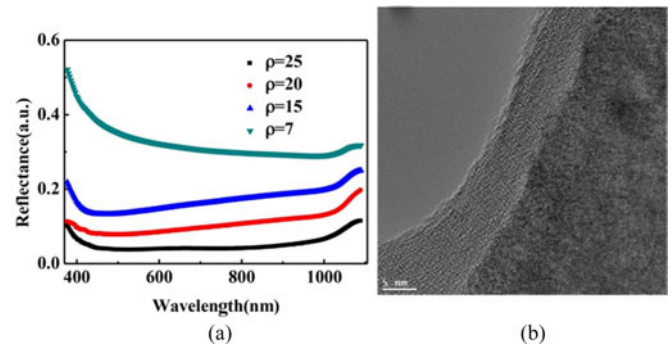


Fig. 2. (a) Reflection spectra of mc-Si samples after MCCE for  $\rho = 25, 20, 15$ , and 7 in the wavelength range of 375–1075 nm. (b) HR-TEM image collected at a local surface of the nanobowls.

and the gradient refractive index effect of the nanostructures (MCCE texture) with lateral sizes ranging from 30 to 200 nm. It was worth noting that the additive nanobowl-like structures with depth well below 50 nm [see Fig. 1(c)] could help to lower average reflectance of the acidic texture from 31.93% to 16.80%. This value is low enough because the subsequent ARC has not been taken into account. The one-step MCCE with  $\rho$  around 15% was, therefore, selected as the preferential recipe to deliver nanobowl/microbowl dual structures for the potential advantages of increased light harvesting and mitigated surface recombination loss. To further investigate the surface quality, an HR-TEM image was randomly collected at the local surface of the nanobowls, as shown in Fig. 2(b). The HR-TEM image was done after 3-min  $\text{HNO}_3$  treatment. The HR-TEM image representatively showed that the surface was atomically smooth and the crystalline structure maintained perfect instead of the quite rough surfaces in previously reported MCCE processes, suggesting that the Ag-related MCCE process at the condition of  $\rho = 15\%$  does have a strong polishing effect on the Si surface. The surface defect density of the nanobowls is, thus, considered to be highly suppressed.

As well known, it is still a big challenge for industry to achieve a good passivation on nanotextured Si surface utilizing conventional PECVD- $\text{SiN}_x$  because the uniform  $\text{SiN}_x$  layer can rarely be conformably coated on the structures with high aspect ratio. Fortunately, this obstacle does not exist in our case. Fig. 3(a)–(c) showed the SEM images of acidic texture, acidic texture with conventional two-step MCCE texture (conventional black-Si structure), and acidic texture with our nanobowl/microbowl dual structure, respectively, all coated with an 80-nm  $\text{SiN}_x$  layer. One could clearly see that the uniform  $\text{SiN}_x$  layer can only be conformably coated on both the surfaces of the acidic texture [see Fig. 3(a)] and the nanobowl/microbowl dual structure [see Fig. 3(c)], but not the conventional black-Si structure. Additionally, the effective minority carrier lifetime ( $\tau_{eff}$ ) measurement using microwave photoconductivity decay was employed to evaluate the surface/interface defects, which greatly influenced the photovoltaic characteristics. The scanned lifetime images on total area ( $156 \times 156 \text{ mm}^2$ ) of the three samples with only front-sided  $\text{SiN}_x$  coating were shown in Fig. 3(d)–(f), respectively. Although the samples used for characterizations of



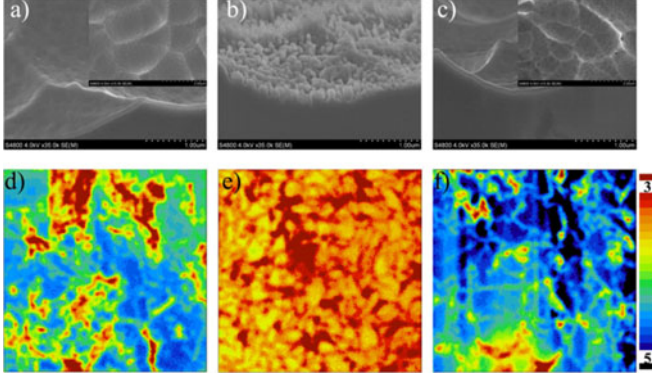


Fig. 3. (a)–(c) SEM images and (d)–(f) minority carrier lifetime mapping of standard acidic texture, conventional black-Si structure, and nanobowl/microbowl dual structure after coated with  $\text{SiN}_x$ . The insets in (a) and (c) are top-viewed SEM images.

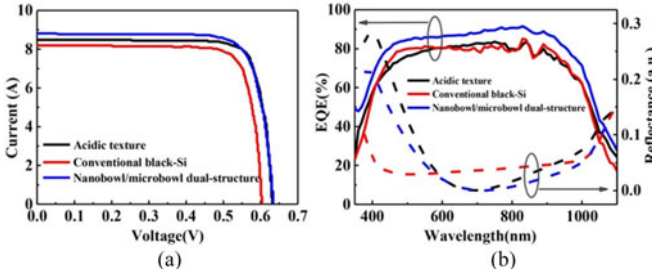


Fig. 4. (a) and (b) Current–voltage ( $I$ – $V$ ), EQE characteristics, and reflection spectra of three mc-Si solar cells with standard acidic texture, conventional b-Si, and acidic texture with our nanobowl/microbowl dual structure.

TABLE I  
PHOTOVOLTAIC PROPERTIES OF THE THREE TYPES OF MC-SI SOLAR CELLS

	$V_{oc}$ (V)	$I_{sc}$ (A)	$FF$	$E_{ff}$ (%)
Acidic texture	0.631	8.481	0.804	17.70
b-Si	0.603	8.188	0.795	16.15
Micro/nano dual structure	0.633	8.817	0.794	18.23

$\tau_{eff}$  were not strictly symmetrical configuration with double-sided coatings, the surface recombination properties can still be indirectly evaluated by measuring the  $\tau_{eff}$ , while the thickness of device was constant. The averaged  $\tau_{eff}$  for the samples of acidic texture, conventional black-Si structure, and the nanobowl/microbowl samples were 4.018, 3.287, and 4.495  $\mu\text{s}$ , respectively. Our nanobowl/microbowl dual structure showed the highest  $\tau_{eff}$  with the best uniformity even in comparison with the standard acidic texture. This could be attributed to the effective reduction of the surface defects and the creation of atomically smooth Si surfaces, which was also supported by TEM observation.

All structures were fabricated into solar cells with the standard alumina back-surface-field configuration, and the current–voltage ( $I$ – $V$ ) curves and EQE spectra were shown in Fig. 4. Photovoltaic characteristics were summarized in Table I, while statistical parameters were shown in Fig. 5.

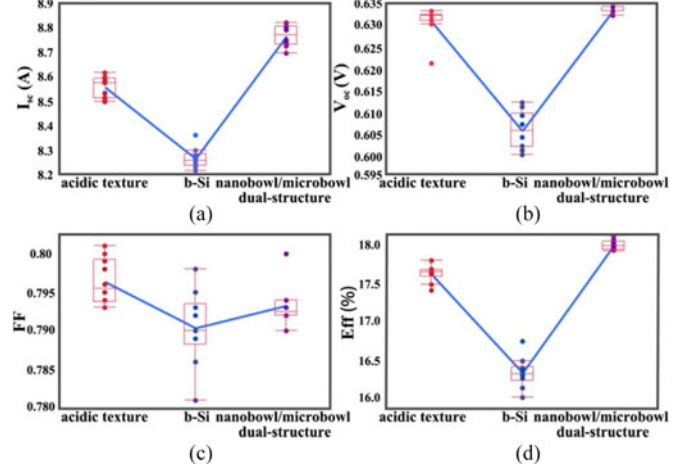


Fig. 5. Electrical parameters statistically collected from a large quantities of mc-Si solar cells with the three different surface textures in a standard production line.

It was evident that the conversion efficiency ( $\eta$ ) and the short-circuit current ( $I_{sc}$ ) of solar cell fabricated by our one-step MCCE method were much higher than the other two kinds of samples, while the open-circuit voltage ( $V_{oc}$ ) keeps identical. The medium fill factor ( $FF$ ) of our novel one-step MCCE sample might attribute to the contaminations originated from the processing. As shown in Fig. 4(b), the poor  $I_{sc}$  of the two-step MCCE texture stemmed from the low quality of passivation, as well as the deteriorated light-harvesting properties at the wavelengths beyond 600 nm that was caused by the ARC coating [see Fig. 3(b)], whereas its deep nanopores would lead to severe leakage problem and, thus, result in poor  $V_{oc}$  and  $FF$ . The better EQE performance in the whole wavelength range of our improved one-step MCCE sample further demonstrated its superiorities in light trapping and surface passivation, echoing with the pronounced improved  $\eta$  of 18.23%. The inconsistency between the curves of EQE and reflection for conventional black-Si and our nanobowl/microbowl dual structures at short- and long-wavelength regions can be ascribed to the serious surface recombination arising from the greatly enlarged surface area at front and rear surface, as well as the poor front  $\text{SiN}_x$  coating, due to the deep and dense nanostructures on both sides of the black-Si that were formed during the MCCE process. Compared with the solar cells with conventional acidic texture, the cells with nanobowl/microbowl structures showed average enhancements in  $V_{oc}$ ,  $I_{sc}$ , and  $\eta$  of 0.4%, 2.4%, and 2.3%, respectively.

#### IV. CONCLUSION

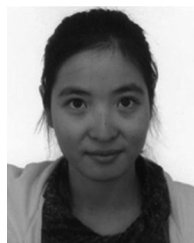
In summary, we have demonstrated an improved MCCE method for fabricating black mc-Si solar cells with efficiency up to 18.23%. The novel nanobowl/microbowl surface structures enabled excellent antireflection, polished surfaces and conformal coating of  $\text{SiN}_x$ , giving rise to a concurrent improvement in electrical and optical characteristics of the solar cells. As a result, the novel MCCE textured mc-Si solar cells had about a 336  $\text{mA}\cdot\text{cell}^{-1}$  increase in the short-circuit current density and no decrease in open-circuit voltage compared with the regular

acidic textured mc-Si solar cell. More importantly, the highly simplified MCCE technology might provide huge cost effectiveness in manufacturing high-performance mc-Si for the photovoltaic industry.

## REFERENCES

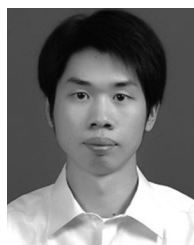
- [1] F. Bai *et al.*, "One-step synthesis of lightly doped porous silicon nanowires in HF/AgNO<sub>3</sub>/H<sub>2</sub>O<sub>2</sub> solution at room temperature," *J. Solid State Chem.*, vol. 196, pp. 596–600, Dec. 2012.
- [2] B. Dou *et al.*, "Fabrication of ultra-small texture arrays on multicrystalline silicon surface for solar cell application," *Sol. Energy*, vol. 91, pp. 145–151, May 2013.
- [3] S. Liu *et al.*, "Improvement of conversion efficiency of multicrystalline silicon solar cells by incorporating reactive ion etching texturing," *Sol. Energy Mater. Sol. C*, vol. 127, pp. 21–26, Aug. 2014.
- [4] B. K. Nayak, V. V. Iyengar, and M. C. Gupta, "Efficient light trapping in silicon solar cells by ultrafast-laser-induced self-assembled micro/nano structures," *Prog. Photovoltaics, Res. Appl.*, vol. 19, no. 6, pp. 631–639, Jan. 2011.
- [5] K. M. Park, M. B. Lee, J. H. Jung, and S. Y. Choi, "Fabrication and characteristics of mc-Si solar cells with RIE-textured surface," *Mol. Crystals Liquid Crystals*, vol. 565, no. 1, pp. 115–123, Aug. 2012.
- [6] S. Zhong *et al.*, "Influence of the texturing structure on the properties of black silicon solar cell," *Sol. Energy Mater. Sol. C*, vol. 108, pp. 200–204, Jan. 2013.
- [7] A. K. Volk *et al.*, "Honeycomb structure on multi-crystalline silicon Al-BSF solar cell with 17.8% efficiency," *IEEE J. Photovoltaics*, vol. 5, no. 4, pp. 1027–1033, Jul. 2015.
- [8] S. Jeong *et al.*, "Hybrid silicon nanocone-polymer solar cells," *Nano Lett.*, vol. 12, no. 6, pp. 2971–2976, Apr. 2012.
- [9] J. Oh, H. C. Yuan, and H. M. Branz, "An 18.2%-efficient black-silicon solar cell achieved through control of carrier recombination in nanostructures," *Nat. Nanotechnol.*, vol. 7, pp. 743–748, Sep. 2012.
- [10] J. Zhang *et al.*, "A 12%-efficient upgraded metallurgical grade silicon-organic heterojunction solar cell achieved by a self-purifying process," *ACS Nano*, vol. 8, no. 6, pp. 11369–11376, Nov. 2014.
- [11] S. Zhong *et al.*, "High-efficiency nanostructured silicon solar cells on a large scale realized through the suppression of recombination channels," *Adv. Mater.*, vol. 27, no. 3, pp. 555–561, Jan. 2015.
- [12] P. Gao *et al.*, "Efficient light trapping in low aspect-ratio honeycomb nanobowl surface texturing for crystalline silicon solar cell applications," *Appl. Phys. Lett.*, vol. 103, Dec. 2013, Art. no. 253105.
- [13] H. C. Yuan *et al.*, "Efficient black silicon solar cell with a density-graded nanoporous surface: Optical properties, performance limitations, and design rules," *Appl. Phys. Lett.*, vol. 95, art. no. 123501, Sep. 2009.
- [14] Z. Yue *et al.*, "Large-scale black multi-crystalline silicon solar cell with conversion efficiency over 18%," *Appl. Phys. A, Mater.*, vol. 116, no. 2, pp. 683–688, Aug. 2014.
- [15] X. Ye *et al.*, "18.45%-efficient multi-crystalline silicon solar cells with novel nanoscale pseudo-pyramid texture," *Adv. Funct. Mater.*, vol. 24, no. 42, pp. 6708–6716, Aug. 2014.
- [16] X. X. Lin *et al.*, "Realization of improved efficiency on nanostructured multicrystalline silicon solar cells for mass production," *Nanotechnology*, vol. 26, no. 12, May 2015, Art. no. 125401.
- [17] F. Toor, J. Oh, and H. M. Branz, "Efficient nanostructured 'black' silicon solar cell by copper-catalyzed metal-assisted etching," *Prog. Photovoltaics, Res. Appl.*, vol. 23, no. 10, pp. 1375–1380, Nov. 2015.
- [18] C. Y. Chen, Y. R. Liu, J. C. Tseng, and P. Y. Hsu, "Uniform trench arrays with controllable tilted profiles using metal-assisted chemical etching," *Appl. Surf. Sci.*, vol. 333, pp. 152–156, Apr. 2015.
- [19] C. Q. Lai, H. Cheng, W. K. Choi, and C. V. Thompson, "Mechanics of catalyst motion during metal assisted chemical etching of silicon," *J. Phys. Chem. C*, vol. 117, no. 40, pp. 20802–20809, Sep. 2013.
- [20] Y. Liu, W. Sun, Y. Jiang, and X. Z. Zhao, "Fabrication of bifacial wafer-scale silicon nanowire arrays with ultra-high aspect ratio through controllable metal-assisted chemical etching," *Mater. Lett.*, vol. 139, pp. 437–442, Jan. 2015.
- [21] F. Bai *et al.*, "Metal-assisted homogeneous etching of single crystal silicon: A novel approach to obtain an ultra-thin silicon wafer," *Appl. Surf. Sci.*, vol. 273, pp. 107–110, May 2013.
- [22] H. Lin *et al.*, "Developing controllable anisotropic wet etching to achieve silicon nanorods, nanopencils and nanocones for efficient photon trapping," *J. Mater. Chem. A*, vol. 1, pp. 9942–9946, Jun. 2013.

- [23] C. Chartier, S. Bastide, and C. Lévy-Clément, "Metal-assisted chemical etching of silicon in HF-H<sub>2</sub>O<sub>2</sub>," *Electrochim. Acta*, vol. 53, no. 17, pp. 5509–5516, Jul. 2008.



**Zhiqin Ying** received the B.S. degree in materials physics from Nanchang University, Nanchang, China, in 2013. She is currently working toward the master's degree with the School of Materials engineering, College of New Energy, Ningbo Institute of Materials Technology and Engineering, Chinese Academy of Sciences, Ningbo, China.

Her research interests include the advanced light-trapping designs for nanostructured solar cells and novel crystalline silicon solar cell process toward industrial application.



**Mingdun Liao** received the B.S. degree in microelectronics and the master's degree in condensed matter physics from Shandong University, Shandong, China, in 2006 and 2009, respectively.

He is currently an Engineer with the Ningbo Institute of Materials Technology and Engineering, Chinese Academy of Sciences, Ningbo, China. His current research interests include the novel crystalline silicon solar cell process toward industrial application.



**Xi Yang** received the B.S. degree in control and instrument specialty from China Jiliang University, Hangzhou, China, in 2008, and the Ph.D. degree in optics from Nankai University, Tianjin, China, in 2013.

He is currently a Research Assistant with the Ningbo Institute of Materials Technology and Engineering, Chinese Academy of Sciences, Ningbo, China. His research interests include the advanced light-trapping designs for nanostructured solar cells.



**Can Han** received the B.S. and master's degrees in nonferrous metallurgy from Central South University, Changsha, China, in 2010 and 2013, respectively.

She is currently an Engineer with the Institute of New Energy Technology, Ningbo Institute of Materials Technology and Engineering, Chinese Academy of Sciences, Ningbo, China. She has authored and coauthored six scientific articles and holds three patents. Her current research interests include the development of high-efficiency photovoltaic technology and relevant instruments.



**Jingqi Li** received the Ph.D. degree in electrical and electronic engineering from Nanyang Technological University, Singapore, in 2006.

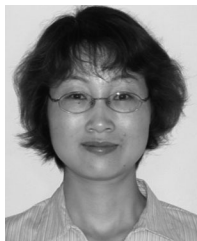
He is currently the Leader of the Thermal and Deposition in Nanofabrication and Thin Film Laboratory, King Abdullah University of Science and Technology, Thuwal, Saudi Arabia. His research interests include carbon nanotube and graphene electronics.



**Junshuai Li** received the B.S. and Ph.D. degrees in physics from Lanzhou University, Lanzhou, China.

He has been a Professor with the School of Physical Science and Technology, Lanzhou University, since December 2012. He performed research on the preparation of high-quality photovoltaic (PV) materials and structures and the design and fabrication of advanced Si nanostructure-based PV devices with Saitama University, Saitama, Japan, from December 2006 to September 2008, and Nanyang Technological University, Singapore, from September 2008 to

March 2012. His main research interests include optical and electrical behaviors in subwavelength semiconductor structures and renewable energy devices.



**Yali Li** received the bachelor's and master's degrees in science from Lanzhou University, Lanzhou, China, and the Doctor degree in engineering from Saitama University, Saitama, Japan.

From January 2009 to March 2012, she was a Research Fellow with Nanyang Technological University, Singapore. She currently holds a faculty position with the School of Physical Science and Technology, Lanzhou University. Her current research interests include high-performance Si nanostructure-based solar cells.



**Pingqi Gao** received the S.B. and Sc.D. degrees from Lanzhou University, Lanzhou, China, in 2002 and 2010, respectively.

From 2007 to 2011, he was with Nanyang Technological University as a Visiting Researcher and a Research Staff in 2011. After that, he joined Fengfan Solar Energy Co., Ltd., as a Chief Technology Officer. In 2013, he joined the Ningbo Institute of Materials Technology and Engineering, Chinese Academy of Sciences, Ningbo, China, as an Associate Professor and became a Professor at the end of 2015, where

he is primarily involved in research into high-efficiency thin crystalline silicon solar cell technology and novel heterojunction and hybrid solar cell technology. He has published more than 40 journal papers and serves as an active referee for 20 journals.

Dr. Gao received an award from the "Thousand Young Talents Program of Zhejiang Province" in 2015.



**Jichun Ye** received the B.S. degree in materials science and engineering from the University of Science and Technology of China, Hefei, China, in 2001 and the Ph.D. degree in materials science from the University of California, Davis, CA, USA, in 2005.

He was a Senior Engineer with Spansion Inc., Calisolar Inc., and Alta Devices Inc. from February 2006 to July 2012. Since August 2012, he has been a Professor and Ph.D. advisor with the Ningbo Institute of Material Technology and Engineering, Chinese Academy of Sciences, Ningbo, China. He has

published more than 30 publications with nearly 500 citations and holds more than 40 patents (including six awarded patents). His research interests include the development of high-efficiency solar cells and the associated processing equipment.

Dr. Ye received an award from the "Thousand Young Talents Program of China" in 2012.